Long-term evolution of the spectral content of continuous seismo-volcanic signals from a network-based analysis

Emmanuel Caballero[1], Nikolai Shapiro[1], Cyril Journeau[1], Léonard Seydoux[2], Jean Soubestre[1], Andrés Barajas[1]

1 University of Grenoble, Institut des Sciences de la Terre, Grenoble, France
2 University Paul Sabatier, Institut de Physique du Globe de Paris, Paris, France

Contact: emmanuel.caballero-leyva@univ-grenoble-alpes.fr

Abstract

Volcanoes are multi-physics systems where different phenomena interact, such as magma transport, degassing, and pressure-induced faulting. These interactions create a series of seismic signals, which characteristics are still under discussion, e.g., their precise origin. In this regard, network-based methods have been developed to determine the level of wavefield coherence and to characterize different seismicity types from complex continuous signals.

In this work, we analyze eight years of continuous seismic data of Piton de la Fournaise, la Réunion, France, We use a method that build the covariance matrix combining interstation single-component cross-correlations. We then evaluate its rank through the estimation of the width of its eigen-values distribution, in other terms, the number of independent seismic sources

The resulting distributions of the spectral width show that continuous signals are characterized by multiple narrow spectral peaks clearly observed in the co-eruptive tremors but also during periods without visible volcanic activity. To enhance these peaks, we re-normalize the distribution of spectral width in the frequency and time domains. We observe in the 1-3 Hz frequency band many spectral peaks that remain nearly constant during very long periods. At the same time, we observe a clear difference in the distribution of these frequencies between the co-eruptive and quiet periods and also some significant variations during long-standing eruptions. We suggest that variations of the spectral lines can be related to the properties of seismo-volcanic sources and eventually to the structural changes and, therefore, can be used in volcano monitoring.

1. Monitoring Volcanic Signals in Volcanic Environment

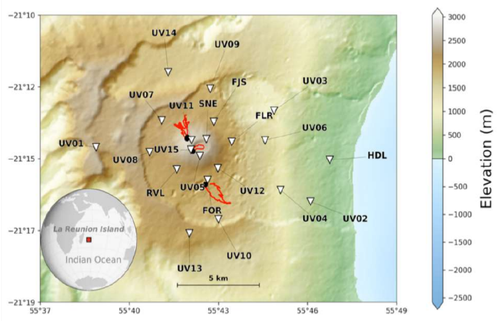

Figure 1. Map of the Piton de la Fournaise volcano, located on the southeast part of La Réunion island, France. The bottom left inset shows La Réunion island location in the Indian Ocean. White inverted triangles represent seismic stations used in this study. Black dots show the eruptive fissure positions corresponding to the January, October, and December 2010 eruptions. Red lines correspond to the lava flows associated with these eruptions. (Modified from Journeau et al., 2022).

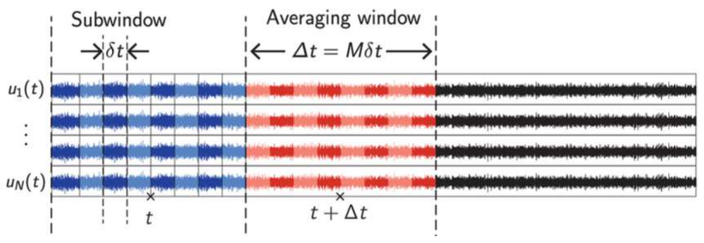

Figure 2. Example of continuous data and the applied windowing. (Figure from Seydoux et al., 2016).

$$\mathbf{C}(f) = \langle \mathbf{u}(f)\mathbf{u}^{\dagger}(f) \rangle = \frac{1}{M} \sum_{m=1}^{M} \mathbf{u}_m(f)\mathbf{u}_m^{\dagger}(f)$$

Array Covariance Matrix

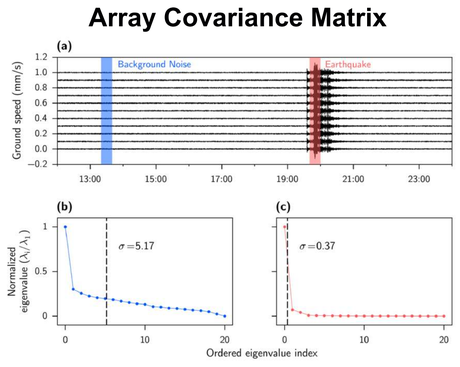

Figure 3. Example of covariance matrix spectra computed from real records (shown in (a)). (b) Covariance matrix spectrum for noise. (c) Covariance matrix spectrum for signal. Values of the covariance matrix spectral width σ are indicated with vertical dashed lines. (Figure from Seydoux et al. 2016).

Covariance matrix Spectral width

$$\sigma(f) = \frac{\sum_{i=1}^{N}(i-1)\lambda_i(f)}{\sum_{i=1}^{N}\lambda_i(f)}$$

Figure 4. Example of covariance matrix spectral width for the 2017 eruption in Piton de la Fournaise. It is worth mentioning the almost continuous spectral peak lines during the eruption. (Figure from Journeau 2022).

Almost continuous spectral lines. What are these signals?

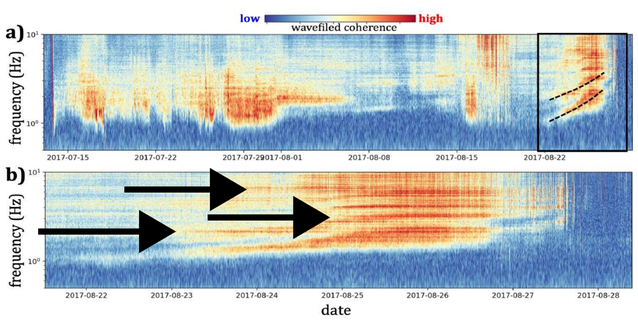

2. Normalization process of the spectral covariance matrix

Figure 5. Covariance matrix spectral width for 2015. We use an Averaging window of 1 hour and 20 sub windows. We observe a hidden signal between inter-eruption periods.

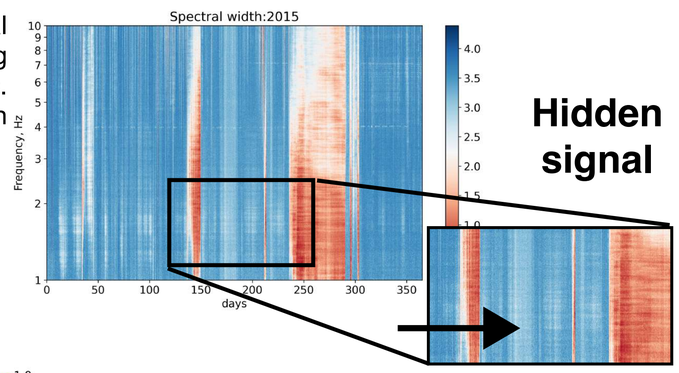

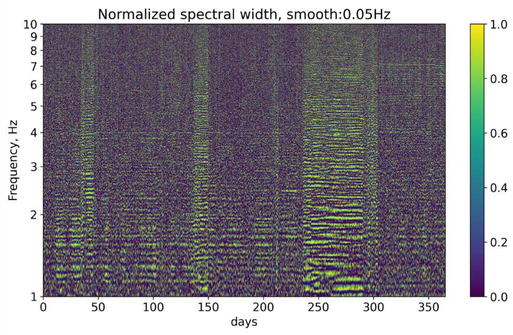

Figure 6. Normalized Covariance matrix spectral width for 2015. The normalization is as follows: i) First we independently smooth each spectral window (0.05 Hz), ii) we calculate the upper envelope, ii) we subtract the upper envelope from the original spectral width, iv) we calculate a new upper envelope, v) we define a threshold for which the new spectral width is equal to zero, and vi) we divide the new spectral width by the new upper envelope.

Figure 7. Covariance matrix spectral width after filtering in time. We use a Wiener filter of 6 hours to enhance the signal. We now focus only in the 1-3 Hz frequency band. We distinguish a signal corresponding to eruptions and a signal present during inter-eruption periods.

Inter-eruption periods
Eruptions

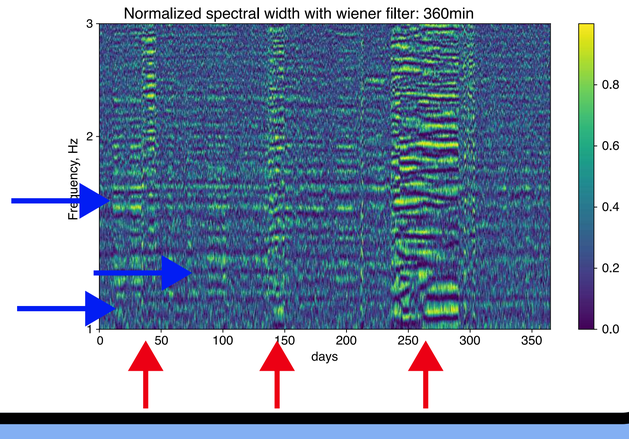

3. Clustering of normalized spectral width

Figure 8. Correlation coefficient *CC* matrix for the 2015 normalized spectral width

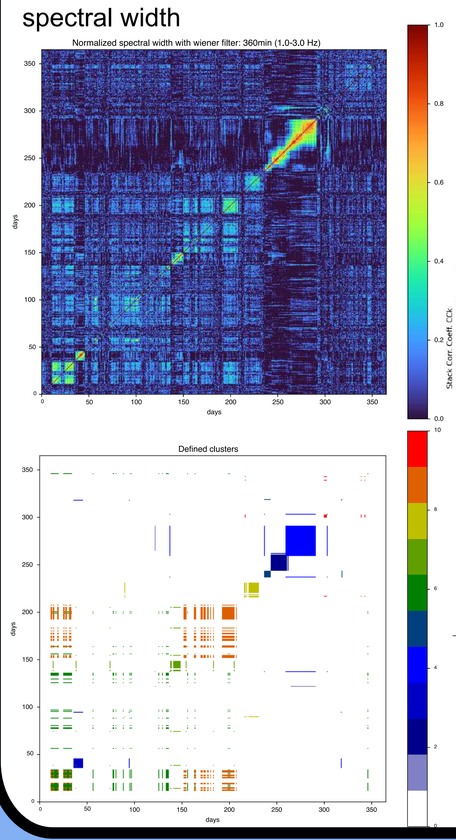

Figure 9. Creation of clusters from correlation coefficient matrix following Soubestre et al. (2018). (a) Stacking of the *CC* matrix. The maximum of the stacking is shown as black dashed lines. (b) Time window of the *CC* matrix corresponding to the maximum of the stacking of the correlation coefficient. The threshold of 0.3 is shown as red dashed lines. The time windows over this threshold are taken as part of the cluster. (c) Correlation coefficient matrix without the cluster time windows.

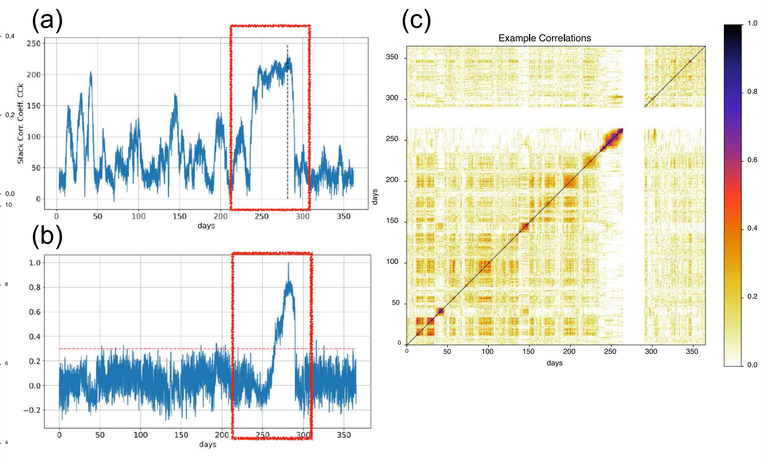

Figure 10. Defined clusters for the 2015 correlation coefficient matrix. Each color represents a different cluster.

4. Long-term evolution of spectral width templates

Figure 11. Individual normalized spectral width templates. Each template is built with the normalized spectral width time windows that corresponds to each cluster

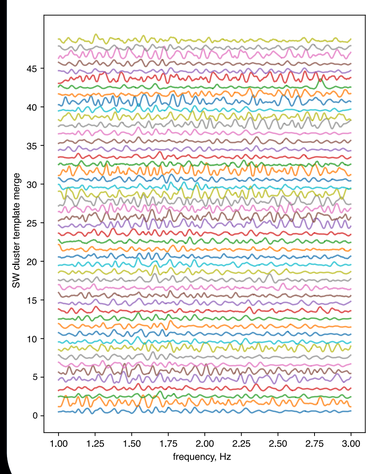

Figure 12. Long-term evolution of the normalized spectral width cluster templates. (a) Evolution of correlation coefficient for each cluster time series from 2011 to 2020. (b) Number of detections for each cluster.

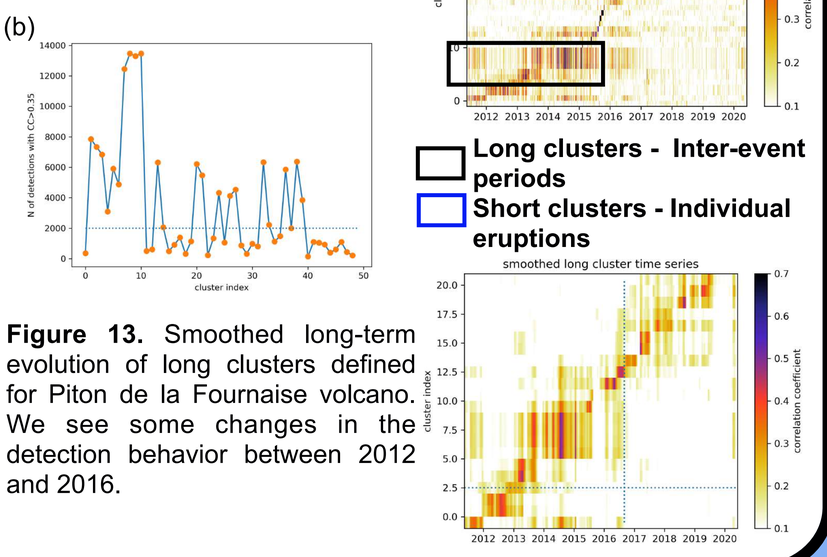

Long clusters - Inter-event periods
Short clusters - Individual eruptions

Figure 13. Smoothed long-term evolution of long clusters defined for Piton de la Fournaise volcano. We see some changes in the detection behavior between 2012 and 2016.

Conclusions

For the period of 2011 to 2020, we characterize the Piton de la Fournaise volcano using the covariance matrix spectral width. We use a new methodology to normalized the covariance matrix spectral width and compute the corresponding correlation coefficient matrix between time windows. We cluster the correlation coefficient matrix and find two different types of clusters, short clusters related to volcanic eruptions, and long clusters related to long-term inter-eruption periods.

We suggest that these clusters could be used to track changes in the volcanic system, and volcano monitoring.

References

Journeau, C., Shapiro, N. M., Seydoux, L., Soubestre, J., Ferrazzini, V., & Peltier, A. (2020). Detection, classification, and location of seismovolcanic signals with multicomponent seismic data: example from the Piton de La Fournaise Volcano (La Réunion, France). Journal of Geophysical Research: Solid Earth, 125(8), e2019JB019333.

Seydoux, L., Shapiro, N. M., de Rosny, J., Brenguier, F., & Landès, M. (2016). Detecting seismic activity with a covariance matrix analysis of data recorded on seismic arrays. Geophysical Journal International, 204(3), 1430-1442.

Soubestre, J., Shapiro, N. M., Seydoux, L., de Rosny, J., Droznin, D. V., Droznina, S. Y., ... & Gordeev, E. I. (2018). Network-based detection and classification of seismovolcanic tremors: Example from the Klyuchevskoy volcanic group in Kamchatka. Journal of Geophysical Research: Solid Earth, 123(1), 564-582.